HHS Public Access

Author manuscript

Nat Med. Author manuscript; available in PMC 2018 May 20.

Published in final edited form as:

Nat Med. 2018 January ; 24(1): 95–102. doi:10.1038/nm.4448.

Granulocyte-derived TNFα promotes vascular and hematopoietic regeneration in the bone marrow

Emily Bowers[1,2], **Anastasiya Slaughter**[1], **Paul S. Frenette**[3,4], **Rork Kuick**[5], **Oscar M. Pello**[6], and **Daniel Lucas**[1,2,7]

[1]Department of Cell and Developmental Biology. University of Michigan School of Medicine. Ann Arbor. Michigan, USA

[2]Center for Organogenesis, University of Michigan School of Medicine. Ann Arbor. Michigan, USA

[3]Ruth L. and David S. Gottesman Institute for Stem Cell and Regenerative Medicine Research, Albert Einstein College of Medicine, Bronx, New York, USA

[4]Department of Medicine and Department of Cell Biology, Albert Einstein College of Medicine, Bronx, New York, USA

[5]Department of Biostatistics, University of Michigan School of Public Health, Ann Arbor, Michigan, USA

[6]The John Goldman Center for Cellular Therapy, Hammersmith Hospital, Imperial College Healthcare NHS Trust

[7]The University of Michigan Comprehensive Cancer Center, University of Michigan, Ann Arbor, USA

Endothelial cells are a critical component of the bone marrow (BM) stromal network that maintains and regulates hematopoietic cells[1–9]. Vascular regeneration precedes, and is necessary for, successful hematopoietic stem cell (HSC) transplantation, the only cure for most hematopoietic diseases[2,4]. Recent data suggest that mature hematopoietic cells can regulate BM stromal cells function [10–13]. Whether a similar crosstalk regulates the BM vasculature is not known. Here we find that donor hematopoietic cells act on sinusoidal endothelial cells to induce host blood vessel and hematopoietic regeneration after BM transplantation in mice. Adoptive transfer of BM, but not peripheral, granulocytes prevented the death of mice transplanted with limited HSC numbers and accelerated recovery of host vessels and hematopoietic cells. Moreover, selective granulocyte ablation *in vivo* impaired vascular and hematopoietic regeneration after BM transplantation. Gene expression analyses

Correspondence should be addressed to D.L. (dlucasal@med.umich.edu).

Contributions

E.B. and D.L. designed the study; E.B., A.S. and D.L. designed, performed and analyzed experiments. O.M.P. suggested and designed experiments. R.K. performed statistical analyses. P.S.F. provided *Nestin-gfp*, *Tnfa*$^{-/-}$, *Tnfr1*$^{-/-}$ and *Tnfr2*$^{-/-}$ mice and designed experiments, E.B. and D.L. wrote the manuscript with help from all coauthors. D.L. supervised the manuscript.

Competing financial interests

None.

indicated that granulocytes are the main source of the cytokine TNFα, whereas its receptor, TNFR1, is selectively upregulated in regenerating blood vessels. In adoptive transfer experiments, wild-type, but not *Tnfa*$^{-/-}$, granulocytes induced vascular recovery, and wild-type granulocyte transfer did not prevent death or promote vascular regeneration in *Tnfr1*$^{-/-}$*:Tnfr2*$^{-/-}$ mice. Thus, by delivering TNFα to endothelial cells, granulocytes promote blood vessel growth and hematopoietic regeneration. Manipulation of the crosstalk between granulocytes and endothelial cells may lead to new therapeutic approaches to improve blood vessel regeneration and increase survival and hematopoietic recovery after HSC transplantation.

Blood cell production takes place in the bone marrow (BM), where a network of non-hematopoietic stromal cells provides a unique microenvironment that maintains and regulates differentiating hematopoietic cells[14]. The endothelial cells that form the blood vessels of the BM are key constituents of this stromal network, producing angiocrine factors such as CXCL12, SCF, Pleiotrophin, and Notch ligands that regulate hematopoietic stem cells and progenitors[1,6–9,15,16] and other stromal cells[6]. Endothelial cells also play a critical role after HSC transplantation by producing angiocrine factors that promote hematopoietic regeneration[1,3,4,16,17]. The myeloablative treatments used to eliminate host hematopoietic cells severely damage BM blood vessels[2,4,18], which must regenerate before they can support hematopoiesis[2,4,19]. Therapies that promote vessel survival or regeneration also promote hematopoietic recovery[2,4,19]. Recent studies have shown that mature hematopoietic cells like macrophages[11–13] and peripheral blood neutrophils[10] can regulate the function of BM osteoblastic stromal cells, but it is not known whether mature blood cells also regulate the BM vasculature.

To test whether hematopoietic cells crosstalk with the vasculature in the context of BM transplantation and regeneration, we transplanted different amounts of CD45.2^{+} bone marrow nucleated cells (BMNCs) into lethally irradiated CD45.1^{+} recipient mice. Fourteen days later the transplanted mice showed a dose-dependent increase in the numbers of hematopoietic and CD45^{-}Ter119^{-}CD31^{+}CD105^{+} endothelial cells in the BM (Fig. 1a,b and Supplementary Fig. 1a). To analyze the vascular network of these mice, we injected αCD31 and αCD144 antibodies intravenously, followed by dissection and 3D whole-mount imaging of the sternal vasculature[18]. This allowed us to distinguish between true vessels—those with a perfused lumen—and vascular sheets that appear after vascular injury (Supplementary videos 1 and 2). Mice transplanted with a higher number of BMNCs showed a denser vascular network with more numerous and longer vessels, as compared to mice transplanted with a lower number of BMNCs (Fig. 1c,d and Supplementary videos 1 and 2). In agreement with these results, we found reduced vascular permeability (as measured by Evans Blue extravasation[20]) in mice transplanted with a higher number of donor BMNCs (Fig. 1e). To test whether the endothelial cells observed in the sternal vasculature after transplantation were host or donor derived, we transplanted WT mice with 20×10^{6} BMNCs purified from *Ubc-gfp* mice, which constitutively express GFP in all cells. We did not detect GFP expression in the endothelial cells from the recipients , indicating that virtually all endothelial cells were host derived (Fig. 1f). Transplantation of a higher number of BMNCs led to increased endothelial cell recovery early after transplantation (Supplementary Fig. 1b) and reductions in the fractions of necrotic endothelial cells (Supplementary Fig. 1c), but had

no effect on the cycling of endothelial cells (Supplementary Fig. 1d). These data demonstrate that donor hematopoietic cells promote endothelial cell survival and drive the recovery of a functional, host-derived, vascular network in the recipient mice.

These results were surprising because hematopoietic progenitors have been reported to inhibit vascular regeneration via angiopoietin-1[21]. We thus investigated whether the observed vascular recovery was mediated by hematopoietic cells that are more mature than the progenitors previously investigated. After FACS-purifying CD45.2$^+$ hematopoietic cells into subpopulations based on the expression of mature lineage markers, we adoptively transferred each of these subpopulations, together with 10^5 CD45.1$^+$ BMNC (as a source of donor HSCs), into γ-irradiated CD45.2$^+$ recipients; each subpopulation was transplanted at the same ratio as it is present *in vivo*. Since adoptively-transferred cells are thought to have limited self-renewal capacity *in vivo*, we adoptively transferred the same populations every 2–3 days for 2 weeks (Fig. 2a). Of the mature cell types tested , only Gr1$^+$CD115$^-$ granulocytes, which contain all BM neutrophils and late neutrophil progenitors[11], were capable of inducing rapid recovery of endothelial cells (Fig. 2b). Notably, granulocyte transfer also promoted survival of the recipient mice (Fig. 2c) and led to faster recovery of hematopoietic cells in the periphery (Fig. 2d). In agreement with previous studies[2,4,19] that demonstrated a strong correlation between endothelial cell recovery and survival, we found that moribund mice showed less vascular recovery (Supplementary Fig. 2a). Imaging of the sternal vasculature showed that granulocyte-treated mice had more blood vessels than PBS-treated controls or mice transferred with monocyte/macrophages, lymphocytes or erythroid-lineage cells (Fig. 2e,f). Granulocyte transfer also rescued vascular leakiness in irradiated mice, but only when transferred at very high doses (Fig. 2g). Granulocyte-induced recovery was not mediated by induction of systemic inflammation, as we did not detect significant increases in inflammatory cytokine levels in BM or plasma (Supplementary Fig. 2b); injury to peripheral tissues, as assessed by pathology analyses (Supplementary Fig. 2c); or increased granulocyte recruitment to peripheral tissues (Supplementary Fig. 2d). We also did not find increased endothelial cell recovery in peripheral tissues in granulocyte-treated mice (Supplementary Fig. 2e).

Transfer of common myeloid progenitors can protect lethally irradiated mice from death until the few host HSC that survive irradiation can restore hematopoiesis[22]. To test if granulocytes induce survival through a similar mechanism, we adoptively transferred granulocytes without accompanying BMNCs into lethally irradiated mice. In the absence of donor hematopoietic stem and progenitor cells (HSPCs), granulocytes were not capable of rescuing irradiation-induced death (Supplementary Fig. 2f).

Next, we performed granulocyte transfer together with BMNCs and followed vascular and hematopoietic recovery up to 4 weeks after transplantation (Fig. 2h and Supplementary Fig. 3a,b). These analyses revealed that compared to BMNCs alone, granulocyte transfer promoted endothelial cell survival early after transplantation, as evidenced by reduced numbers of apoptotic and necrotic endothelial cells (Fig. 2i); this endothelial protection was comparable to that induced by transfer of a high number of BMNCs (Supplementary Fig. 1c). Moreover, we found that granulocytes induced expression of *Cflar* (also known as *cFlip)*, which encodes an antiapoptotic prosurvival factor[23], in BM endothelial cells *in vivo*

(Supplementary Fig. 3c). In contrast granulocytes did not induce expression of hematopoietic supportive molecules such as *Cxcl12*, *Scf*, or Notch ligands, or lead to activation of *Hif1a* or its downstream targets (Supplementary Fig. 3d-f). These results indicate that granulocytes promote endothelial cell survival.

To further analyze the effect of granulocytes on hematopoietic recovery, we performed lineage tracing experiments (Supplementary Fig. 4a). In granulocyte-treated mice, the increase in peripheral blood and BM hematopoietic recovery was associated with persistence of the transferred BM granulocytes (Supplementary Fig. 4d,g) and increased production of host cells (Supplementary Fig. 4c-h). Notably, adoptive transfer of peripheral blood neutrophils, which home to the bone marrow and crosstalk with CXCL12 abundant reticular stromal cells to regulate HSC trafficking[10], did not induce vascular or hematopoietic recovery (Supplementary Fig. 4b-h), and, in contrast to BM granulocytes, did not persist in the recipient mice (Supplementary Fig. 4d,g). We hypothesized that increased vascular recovery might facilitate engraftment of donor-derived HSPCs. To test this concept we performed competitive transplants. We FACS-purified donor $CD45.1^+$ cells from primary recipients which had been transplanted with or without granulocytes and transplanted the $CD45.1^+$ cells, together with competitor $CD45.1^+$:$CD45.2^+$ BMNCs, into lethally irradiated $CD45.2^+$ secondary recipients (Fig. 2a). Mice transplanted with $CD45.1^+$ BMNCs from granulocyte-treated mice displayed increased short-term T- and myeloid cell, but not long-term (16 weeks) multilineage, $CD45.1^+$ cell contribution to the peripheral blood (Fig. 2j). These indicate that granulocyte-induced vascular recovery promotes engraftment of short-lived, lineage-committed, hematopoietic progenitors but not HSC. Taken together, these results demonstrate that adoptive transfer of BM granulocytes is sufficient to promote survival and drive vascular and hematopoietic cell recovery after myeloablation, without exhausting the donor HSC pool.

Next, to test whether granulocytes produced by BMNC transplantation promote vascular regeneration, we bred *Mrp8-cre-IRES-GFP* mice, in which Cre expression is largely restricted to granulocytes and a fraction of granulocyte monocyte progenitors (GMP), with *iDTR* mice, in which the diphtheria toxin receptor (DTR) is induced by Cre-mediated recombination. We transplanted lethally irradiated recipients with 5×10^6 BMNCs purified from *iDTR* or *Mrp8-cre-IRES-GFP:iDTR* mice, followed by DT treatment. This strategy led to efficient granulocyte ablation in the recipient mice transplanted with *Mrp8-cre-IRES-GFP:iDTR*, but not control *iDTR*, BMNCs (Fig. 3a,b). In the mice transplanted *with Mrp8-cre-IRES-GFP:iDTR* BMNCs, granulocyte ablation led to impaired vascular regeneration and increased vascular leakage (Fig. 3c-e) and impaired peripheral blood cell recovery (Fig. 3f), as well as reduced numbers of monocytes and macrophages in the BM (Fig. 3g-i). To confirm that the monocyte/macrophage loss was not responsible for the reduced number of blood vessels, we ablated granulocytes *in vivo* by injection of α-Ly6G, an antibody that ablates granulocytes exclusively[24]. Treatment with α-Ly6G, but not an isotype control antibody, depleted granulocytes (Fig. 3j) and impaired vascular regeneration (Fig. 3k), and also caused loss of BM monocytes and lymphocytes (Supplementary Fig. 5a,b). In a complementary approach we transplanted recipient mice with a single graft of total BMNCs or a graft in which the granulocytes were removed prior to transplantation via FACS. As expected, mice transplanted with a granulocyte-depleted graft showed reduced granulocyte

numbers (Fig. 3l) and impaired endothelial and hematopoietic regeneration 6 days after transplantation (Fig. 3m and Supplementary Fig. 5c,d). These experiments demonstrate that donor-derived granulocytes are necessary for efficient vascular regeneration.

To investigate the mechanisms through which granulocytes promote vascular regeneration, we profiled BM granulocytes for the expression of multiple angiogenic factors, as assessed by qPCR. We detected expression of fibroblast growth factor 1 (*Fgf1*), progranulin (*Prgn*), pleiotrophin (*Ptn*), vascular endothelial growth factor A (*Vegfa*) and TNFα (*Tnfa*, Supplementary Fig. 6a). We focused on TNFα because *Tnfa* was enriched in BM granulocytes (Supplementary Fig. 6b), *Tnfr1* (*Tnfrsf1a*, encoding a TNFα receptor) was enriched in endothelial cells as compared to other BM stromal cells (Supplementary Fig. 6c), *Tnfr1* was upregulated in regenerating endothelial cells (Supplementary Fig. 6c) and TNFα induces cFLIP expression[25]. TNFα is a powerful angiogenic factor in mice[26,27] and neutrophil-derived TNFα drives blood vessel formation during zebrafish development[28]. Analyses of $Tnfa^{-/-}$ or $Tnfr1^{-/-}{:}Tnfr2^{-/-}$ mice revealed fewer endothelial cells in the steady-state bone marrow (Supplementary Fig. 7), indicating that TNFα regulates vascular homeostasis.

To test whether TNFα also plays a role in regeneration, we myeloablated WT or $Tnfa^{-/-}$ mice with a single injection of 5-fluorouracil. As compared to WT mice, $Tnfa^{-/-}$ mice displayed reduced numbers of BM endothelial cells and rapidly succumbed to this treatment (Fig. 4a,b). The reduced survival of $Tnfa^{-/-}$ mice suggests a defect in endothelial regeneration, but might also be due to the reduced number of BM endothelial cells in the steady-state. Moreover, injection of recombinant TNFα induced faster vascular recovery in 5-fluorouracil-treated WT and $Tnfa^{-/-}$ mice and delayed death in $Tnfa^{-/-}$ mice (Fig. 4a,b). These results indicate that TNFα is needed for normal BM endothelial cell numbers during homeostasis and that TNFα can directly promote endothelial regeneration.

BM granulocytes expressed the membrane-bound form of TNFα, as assessed by flow cytometry (Supplementary Fig. 8a). To test whether granulocytes promote vascular regeneration specifically via TNFα production, we performed adoptive transfer experiments using granulocytes purified from WT and $Tnfa^{-/-}$ mice. To distinguish between the regenerative effects of granulocytes on sinusoids and arterioles, we used *Nestin-gfp* mice; in this model, Nestin-GFP^{bright} cells label arterioles[18,29]. WT but not $Tnfa^{-/-}$ granulocytes induced sinusoidal vessel recovery, as demonstrated by quantification of endothelial cells by FACS (Fig. 4c) and sinusoidal and arteriolar vessel numbers by 3D whole-mount immunofluorescence (Fig 4d,e). In addition, WT but not $Tnfa^{-/-}$ granulocytes rescued survival of the recipient mice and led to faster white and red blood cell recovery in the peripheral blood (Fig. 4f,g). Imaging analyses showed that, during regeneration, granulocytes preferentially localized to sinusoids: 76% of granulocytes were found within 5μm of a sinusoid, whereas a much smaller fraction (14%) localized to Nestin-GFP^{bright} arterioles (Fig. 4h,i). B lymphocytes, which did not induce regeneration (Fig. 2b), showed fewer interactions with BM vessels than did granulocytes (Supplementary Fig. 8b,c). Granulocyte recruitment to regenerating vessels was independent of CXCR4 and CXCR2 (Supplementary Fig. 8d-f), the major receptors that regulate neutrophil trafficking during homeostasis[30], indicating that other mechanisms regulate granulocyte recruitment to injured

vessels. Adoptive granulocyte transfer failed to promote survival and vascular regeneration in *Tnfr1*$^{-/-}$*:Tnfr2*$^{-/-}$ mice, as compared to control mice, after transplantation (Fig. 4j,k), suggesting that the crosstalk between granulocytes and endothelial cells is direct.

To confirm that granulocyte-derived TNFα does not promote regeneration via effects on hematopoietic cells , we transplanted WT recipients with an initial graft of 10^5 WT or *Tnfr1*$^{-/-}$*:Tnfr2*$^{-/-}$ BMNCs followed by adoptive transfer of WT granulocytes. We found reduced peripheral blood and BM hematopoietic recovery in mice transplanted with *Tnfr1*$^{-/-}$*:Tnfr2*$^{-/-}$ as compared to WT BMNCs (Supplementary Fig. 9a,b), consistent with previous work showing that, during regeneration, TNFα acts on HSPC to promote engraftment[31]. Mice transplanted with *Tnfr1*$^{-/-}$*:Tnfr2*$^{-/-}$ BMNCs also showed delayed vascular regeneration (Supplementary Fig. 9c), associated with a deficit in granulocyte production (Supplementary Fig. 9a). Adoptive transfer of WT granulocytes rescued death (Supplementary Fig. 9d) and dramatically increased vascular and hematopoietic recovery (Supplementary Fig. 9a,b) in mice transplanted with either WT or *Tnfr1*$^{-/-}$*:Tnfr2*$^{-/-}$ BMNCs. These demonstrate that granulocyte-derived TNFα does not act on hematopoietic cells to promote vascular regeneration

Myeloid cells are key players in vascular remodeling and regeneration in many tissues[26,28,32]. Our data demonstrate that granulocytes, the most abundant cells in the BM, interact with the BM microenvironment to drive vascular regeneration specifically via TNFα. Since endothelial cell-derived factors (e.g. Notch ligands, EGF, Pleiotrophin)[1,3,16,17,33] and vessel regeneration[2,4,19] are necessary for hematopoietic recovery, these results suggest the existence of a positive feedback loop after BM injury. In this loop, endothelial cell regeneration drives hematopoietic progenitor proliferation and generation of granulocytes, which in turn support further vessel regeneration. Our results also indicate that granulocytes overcome the inhibition of vascular regeneration induced by hematopoietic progenitors[21]. After transplantation, HSCs and multipotent progenitors preferentially generate myeloid cells[34], a preference believed to satisfy the physiological demand for peripheral neutrophils to prevent infections. Our results suggest that this myeloid bias, by generating granulocytes, might also contribute to recovery by promoting vessel regeneration.

The effects of TNFα on HSPC function are controversial. Some reports suggest that TNFα acts on HSPCs to promote their maintenance in the steady state and engraftment during regeneration[31,35,36]. Other reports suggest that TNFα acts on HSPCs to inhibit their function during homeostasis and that TNFα-receptor blockade prior to transplantation promotes HSPC survival[37,38]. Our results support the notion that TNFα has pro-regenerative effects on HSPCs. Beyond its effects on hematopoietic cells, our results indicate that granulocytes employ TNFα to drive vascular regeneration. Granulocytes also produce other pro-regenerative factors, such as VEGF, which is necessary for BM vascular regeneration[2] and can recruit angiogenic myeloid cells to the heart[32], and pleiotrophin, which promotes hematopoietic recovery by inducing Ras activation in HSPCs[16,17]. Future studies are needed to determine whether these factors cooperate with TNFα in granulocyte-driven regeneration.

Our data suggest that the composition and cellular output of the initial graft affect the recovery of host vessels and hematopoietic cells which may have implications in the context of clinical HSC transplantation. In patients especially vulnerable to myeloablation, such as those with DNA repair defects or those in which the BM stroma has been damaged by prior chemotherapy treatment[39,40], treatment with BM granulocytes could potentially be utilized to ameliorate vascular injury and promote hematopoietic recovery.

Online Methods

Mice

C57BL/6J (CD45.2$^+$) and B6.SJL-*Ptprc^a Pepc^b*/BoyJ (B6.SJL, CD45.1$^+$) were purchased from the Jackson laboratory and bred in-house. C57BL/6j:B6.SJL hybrids (CD45.2$^+$:CD45.1$^+$) were generated by breeding C57BL/6J with B6.SJL mice. *Ubc-gfp* mice[41], *Mrp8-cre-IRES-gfp* (*Mrp8-cre*)[42], *iDTR*[43], *Tnfa$^{-/-}$*[44] mice were originally purchased from the Jackson laboratory. *Tnfr1$^{-/-}$*:*Tnfr2$^{-/-}$*[45] mice were also purchased from the Jackson laboratory and then backcrossed for four additional generations into the C57BL/6J background and then bred in-house. *Nestin-gfp* mice[18,29] were a gift from Paul S. Frenette. All experiments were performed in 8–14 week old male mice. All mice were housed at the SPF facility managed by the Unit for Laboratory Animal Medicine (ULAM) at the University of Michigan. Experiments complied with all relevant ethical regulations and were approved by the Institutional Animal Care and Use Committee at the University of Michigan.

Bone marrow isolation

Mice were euthanized by isoflurane overdose. Bone marrow was harvested by flushing mouse long bones with 1 ml of ice-cold PEB (2mM EDTA 0.5% Bovine serum albumin in PBS). Red blood cells were lysed once by adding 1 mL of RBC Lysis Buffer (NH_4Cl 150mM, $NaCO_3$ 10mM, EDTA 0.1mM). Cells were immediately decanted by centrifugation, resuspended in ice-cold PEB and used in subsequent assays. Due to the known effect of circadian rhythm effects in granulocytes and HSCs[10,46–48], we performed BM harvest at zeitgeber times 3–6 in mice under standard (12h light:12h dark) cycles.

Peripheral blood analyses

Blood was collected from the facial vein in tubes containing EDTA. White blood cell (WBC), red blood cell (RBC) and platelet counts were obtained using an Advia Counter (Siemens) or a Hemavet 950 (Drew Scientific). Prior to flow cytometry staining and analyses, red blood cells in peripheral blood were lysed once by adding 1 mL of RBC Lysis Buffer (NH_4Cl 150mM, $NaCO_3$ 10mM, EDTA 0.1mM). Cells were immediately decanted by centrifugation, resuspended in ice-cold PEB and used in subsequent assays.

Collagenase/Dispase digestion

To purify the stromal cell fraction of the bone marrow (including endothelial cells), we used a modified version of the serial digestion protocol developed by the Simmons laboratory[49]. Digestion buffer was made using 2 mg/ml Collagenase Type IV (Gibco, 17104-019) and 3 mg/ml Dispase (Gibco, 17105-041) dissolved in room temperature PBS. We harvested the

BM by flushing a tibia with 1 ml of digestion buffer into a 5 ml polypropylene snap-cap tube containing another 1 ml of digestion buffer. We mixed the tubes vigorously by hand and incubated at 37°C for 5–7 minutes. Following the first incubation, the tubes were mixed vigorously by hand and then placed back at 37°C for another 5–7 minutes. After this second incubation we collected the supernatant, taking care to leave any macroscopic clumps in the tube. We transferred the digested cells to a tube containing 5 ml of ice-cold PEB. Then we added one ml of digestion buffer to the snap-cap tubes and the process above was repeated until all macroscopic pieces of bone marrow had been digested. The red blood cells were lysed once using RBC Lysis Buffer, filtered through a 100 μm filter (Greiner Bio-one, 542-000), and then immediately spun down in the centrifuge. The cells were resuspended in 1 ml of ice-cold PEB and used for subsequent analyses.

FACS analyses

Cells were stained for 30 minutes in PEB buffer with the indicated antibodies and analyzed in a BD LSRFortessa (BD Biosciences) or FACS-purified using a BD FACS Aria II or a Synergy SY3200 Cell sorter (Sony). Dead cells and doublets were excluded based on FSC and SSC distribution and DAPI (Sigma) exclusion. Data was analyzed using FACS Diva software 8.0 (BDBiosciences). Antibodies used were against B220 (clone RA3-6B2, Cat No: 103224), CD3 (clone 145-2C11, Cat No:100304), CD4 (clone GK1.5, Cat No:100422), CD8 (clone 53-6.7, Cat No:100722), CD11b (clone M1/70, Cat No:101216 or 101204), CD16/32 (clone 93, Cat No:101328), CD19 (clone 6D5, Cat No: 115508), CD31 (clone A20, Cat No:110724), CD41 (clone MWReg30, Cat No:133921 or clone D7, Cat No: 108104), CD45 (clone 30-F11, Cat No:103116), CD45.1 (clone A20, Cat No:110723 or 110708), CD45.2 (clone 104, Cat No:109845, 109823 or 109814), CD105 (clone MJ7/18, Cat No:120410), CD115 (clone AFS98, Cat No:135506 or 135513), CD144 (clone BV13, Cat No: 138006), CD150 (clone TC15-12F12.2, Cat No:115904), F4/80 (clone BM8, Cat No:123122), Gr1 (clone RB6-8C5, Cat No: 108406 or 108404), Ly6-G (clone 1A8, Cat No: 127625), Sca-1 (clone D7, Cat No:108106), Secondary antibody (Goat anti-rat IgG, clone Poly4054, Cat No: 405418), and Ter119 (clone TER-119, Cat No:116220), all from Biolegend, CD117 (clone 2B8, Cat No:105828 and 105833 from Biolegend or 562417 from BD Biosciences), Ki67 (clone SolA15, Cat No:50-5698-82 from ThermoFisher Scientific), Ly6G (clone 1A8, or Cat No: BP0075-1 from Bioxcell) or isotype control (clone 2A3, Cat No: BP0089 from Bioxcell), TNFα (clone MP6-XT22. Cat No: 506303). For cell cycle analyses, cells were first fixed with 4% paraformaldehyde for 20 minutes at 4°C followed by permeabilization of the plasma membrane using 0.1% Triton X-100 for 20 minutes at 4°C. The cells were then stained for 30 minutes in PEB buffer containing 0.1% Triton X-100 with Ki67 (cat No:50-5698-82). Lastly, the cells were incubated in PEB buffer containing DAPI for one hour at room temperature before being analyzed as described above. Apoptotic cells were detected using the CellEvent™ Caspase-3/7 Green Flow Cytometry Assay Kit from Life Technologies (Cat No:C10427). Apoptotic cells were analyzed as described above.

Primary and secondary bone marrow transplantation and adoptive transfer experiments

Recipient male mice were conditioned with two doses of 600 rads using a ^{137}Cs source , 3 hours apart, and immediately transplanted with the indicated amount of donor BMNC (retroorbital injection). For adoptive transfer experiments, the indicated doses of FACS-

purified hematopoietic cells were resuspended in 200μl of PBS and injected retroorbitally into the recipient mice. Due to the known effect of circadian rhythm effects in granulocytes and HSCs[10,46–48], we performed adoptive transfers at zeitgeber times 10–12 in mice under standard (12h light:12h dark) cycles.

In vivo granulocyte ablation

For diphtheria toxin-mediated granulocyte ablation, we treated mice with daily intraperitoneal injections of diphtheria toxin (D0564, Sigma) (0.25μg/mouse/day) for one week starting one week after transplantation. For αLy6G-mediated depletion experiments, we treated mice with 100μg (intraperitoneal) of αLy6G (clone 1A8, BP0075-1, Bioxcell) or isotype control (clone 2A3, BP0089, Bioxcell) at days 1, 3 and 5 after transplantation. Binding of αLy6G prevents staining with αGr1. This prevented the use of Gr1 for detection of granulocytes in αLy6G-injected mice. Thus, in these experiments, $Ly6G^+$ granulocytes were detected by staining BM cells with isotype or αLy6G antibodies: 1μg/ml of αLy6G or isotype antibody was used , followed by staining with a secondary antibody (405418, Biolegend)

5-fluorouracil treatment

We injected mice (retroorbitally) with a single dose of 250mg of 5-fluorouracil (Sigma) per kg of body weight in PBS.

Recombinant TNFα injection

We injected the mice (0.5μg/mouse, intraperitoneally) with recombinant mouse TNFα (718004, Biolegend) daily.

AMD3100 and SBD

AMD3100 (5mg/kg s.c) and SBD (0.3mg/kg, i.p. SB225002, Sigma) were injected intraperitoneally at days 1, 3, and 5 after transplantation and 1 hour before harvest.

Quantification of inflammatory cytokines in plasma and bone marrow extracellular fluid

Inflammatory cytokines were detected using the Legendplex Mouse inflammation panel (740446, Biolegend), following the manufacturer's instructions.

RNA isolation and qPCR analyses

RNA isolation was performed using the Dynabeads mRNA direct kit (Life Technologies) following the manufacturer's instructions. cDNA synthesis was performed using the RNA to cDNA EcoDry Premix (Clontech) following the manufacturer's instructions. qPCR was performed using the SYBR Green Supermix Quanta Biosciences using a ABI PRISM 7900HT Sequence Detection System (Appliedbiosystems). Results were analyzed using SDS 2.4 software (Appliedbiosystems). Oligonucleotides used for amplification are enumerated in Supplementary Table 1.

Whole-mount immunofluorescence analyses

Imaging of the mouse BM sternal vasculature has been described previously[18]. Briefly, mice were injected (retroorbitally) with 5μg of Alexa Fluor 647 anti-mouse CD31 (110724, Biolegend) and 5μg of Alexa Fluor 647 anti-mouse CD144 (138006, Biolegend). Twenty minutes later, mice were euthanized by isoflurane overdose and the sterna retrieved. For each sternum we removed muscle and connective tissue using a scalpel. The sternum was then divided into segments and each segment cut sagitally to expose the BM cavity. Segments were fixed in 4% paraformaldehyde (Sigma) in PBS for 20 minutes at room temperature, washed thrice in PBS and imaged immediately or incubated in blocking solution (20% Goat Serum (Sigma) in PBS) for two hours prior staining with antibodies. Granulocytes or B cells were detected by staining in a solution containing 2.5μg/ml Alexa Fluor 488 anti-mouse Ly6-G (Clone 1A8, Biolegend) or Phycoerythrin conjugated anti-mouse CD19 (Clone 6F5, Biolegend), 5% Goat Serum (Sigma) in PBS for 3 days. Prior to imaging, each segment was glued to 35mm dishes and imaged in a Leica SP5 upright confocal microscope using a 20X, long-distance, water immersion objective, Hybrid detectors, and Leica Application Suite Advanced Fluorescence software. We acquired z-stacks (2.98μm between slices) 20–200μm , depending on the position of the bone. Each slice measured 434.17 in the×axis and 434.17μm in the y axis and was 1024×1024 pixels. All images were acquired at room temperature. For Alexa Fluor 647, the wavelength of the excitation laser was 647 nm and emitted light detected between 660 to 720nm. For Alexa Fluor 488, the wavelength of the excitation laser was 488nm and emitted light detected between 500 to 540nm. For Phycoerythrin, the wavelength of the excitation laser was 560nm and detection from 570 to 600nm. We used Fiji[50] software to generate 3D reconstructions and maximum projections from each image. Blood vessels numbers and length were counted manually in 3D reconstructions in order to be able to distinguish true vessels (with lumen) from vascular sheets (lacking lumen). Composite images of each sternum were assembled by stitching together the maximum projection images in Power Point (Microsoft).

Vascular permeability

Mice received 200 μl of 0.5% Evans Blue Dye (Sigma Aldrich, E2129) in PBS via retro-orbital injection. Thirty minutes later mice were euthanized and perfused with 5 ml of PBS to remove excess Evans Blue from the vessels. To harvest the bone marrow, one femur was flushed with 1 ml of ice-cold PEB. The cells were centrifuged and the supernatant containing the extravasated Evans Blue was removed and placed in a clean 1.5 ml tube. To analyze the amount of Evans Blue in the supernatant, samples were placed in a 96-well plate and read using a Spectramax 340PC from Molecular Devices with the absorbance measured set to 610 nm.

Pathology analyses

Mice were euthanized by isoflurane overdose. Liver, lung, and intestine were removed, processed, embedded in paraffin, sectioned, and stained with hematoxylin/eosin by a necropsy technician in the In-vivo Animal Core (IVAC) at the University of Michigan Medical School. We received the sections and did imaging analysis using an Olympus BX51 with a 20X dry objective lens. Images were captured using a DP-70 digital camera and the

associated software. In-depth pathological analysis was performed by the veterinary pathologist of the IVAC.

Statistics

In most graphs of data, the actual values for each mouse are plotted and the means indicated. In others the means and standard errors are plotted. Sample size was not predetermined and all mice were included in the analyses. Mice were randomly allocated to the different groups based on cage and litter size. For all experiments we aimed to have the same number of mice in the control and experimental groups. For all experiments, at the time of analyses, the investigator was blinded to the group allocation. The only exception was the blood vessel quantification in 3D reconstructions of sternal segments. Statistical differences were calculated using two tailed, Two-sample, T-tests (for experiments with two groups), ANOVA (3 or more groups) on log transformed data, or Log-Rank tests for survival analysis.

Data availability

The primary data that support the results described here are available upon reasonable request. A Life Sciences Reporting Summary is also available.

Supplementary Material

Refer to Web version on PubMed Central for supplementary material.

Acknowledgments

We thank Margot May for excellent technical support. This work was supported by the Pardee Foundation (D.L.). E.B. was funded through a T32 training grant from the Center of Organogenesis at the University of Michigan. We thank Dr. Mark Hoenerhoff and the rest of the UM in vivo core for performing pathology analyses. We thank the mouse imaging laboratory and the flow cytometry core at the University of Michigan for their help with imaging and FACS experiments. R.K., flow cytometry and whole-mount immunofluorescence were partially supported by a core grant from the NIH to the University of Michigan Cancer Center (P30-CA46592).

References

1. Butler JM, et al. Endothelial cells are essential for the self-renewal and repopulation of Notch-dependent hematopoietic stem cells. Cell stem cell. 2010; 6:251–264. [PubMed: 20207228]
2. Hooper AT, et al. Engraftment and reconstitution of hematopoiesis is dependent on VEGFR2-mediated regeneration of sinusoidal endothelial cells. Cell stem cell. 2009; 4:263–274. [PubMed: 19265665]
3. Poulos MG, et al. Endothelial Jagged-1 is necessary for homeostatic and regenerative hematopoiesis. Cell Rep. 2013; 4:1022–1034. [PubMed: 24012753]
4. Doan PL, et al. Tie2(+) bone marrow endothelial cells regulate hematopoietic stem cell regeneration following radiation injury. Stem cells. 2013; 31:327–337. [PubMed: 23132593]
5. Itkin T, et al. Distinct bone marrow blood vessels differentially regulate haematopoiesis. Nature. 2016; 532:323–328. [PubMed: 27074509]
6. Kusumbe AP, et al. Age-dependent modulation of vascular niches for haematopoietic stem cells. Nature. 2016; 532:380–384. [PubMed: 27074508]
7. Greenbaum A, et al. CXCL12 in early mesenchymal progenitors is required for haematopoietic stem-cell maintenance. Nature. 2013; 495:227–230. [PubMed: 23434756]
8. Ding L, Saunders TL, Enikolopov G, Morrison SJ. Endothelial and perivascular cells maintain haematopoietic stem cells. Nature. 2012; 481:457–462. [PubMed: 22281595]

9. Himburg HA, et al. Pleiotrophin regulates the retention and self-renewal of hematopoietic stem cells in the bone marrow vascular niche. Cell Rep. 2012; 2:964–975. [PubMed: 23084748]
10. Casanova-Acebes M, et al. Rhythmic modulation of the hematopoietic niche through neutrophil clearance. Cell. 2013; 153:1025–1035. [PubMed: 23706740]
11. Chow A, et al. Bone marrow CD169+ macrophages promote the retention of hematopoietic stem and progenitor cells in the mesenchymal stem cell niche. The Journal of experimental medicine. 2011; 208:261–271. [PubMed: 21282381]
12. Christopher MJ, Rao M, Liu F, Woloszynek JR, Link DC. Expression of the G-CSF receptor in monocytic cells is sufficient to mediate hematopoietic progenitor mobilization by G-CSF in mice. The Journal of experimental medicine. 2011; 208:251–260. [PubMed: 21282380]
13. Winkler IG, et al. Bone marrow macrophages maintain hematopoietic stem cell (HSC) niches and their depletion mobilizes HSCs. Blood. 2010; 116:4815–4828. [PubMed: 20713966]
14. Morrison SJ, Scadden DT. The bone marrow niche for haematopoietic stem cells. Nature. 2014; 505:327–334. [PubMed: 24429631]
15. Winkler IG, et al. Vascular niche E-selectin regulates hematopoietic stem cell dormancy, self renewal and chemoresistance. Nature medicine. 2012; 18:1651–1657.
16. Himburg HA, et al. Pleiotrophin regulates the expansion and regeneration of hematopoietic stem cells. Nature medicine. 2010; 16:475–482.
17. Himburg HA, et al. Pleiotrophin mediates hematopoietic regeneration via activation of RAS. J Clin Invest. 2014
18. Kunisaki Y, et al. Arteriolar niches maintain haematopoietic stem cell quiescence. Nature. 2013; 502:637–643. [PubMed: 24107994]
19. Poulos MG, et al. Endothelial-specific inhibition of NF-kappaB enhances functional haematopoiesis. Nat Commun. 2016; 7:13829. [PubMed: 28000664]
20. Radu M, Chernoff J. An in vivo assay to test blood vessel permeability. J Vis Exp. 2013:e50062. [PubMed: 23524912]
21. Zhou BO, Ding L, Morrison SJ. Hematopoietic stem and progenitor cells regulate the regeneration of their niche by secreting Angiopoietin-1. eLife. 2015; 4
22. Na Nakorn T, Traver D, Weissman IL, Akashi K. Myeloerythroid-restricted progenitors are sufficient to confer radioprotection and provide the majority of day 8 CFU-S. J Clin Invest. 2002; 109:1579–1585. [PubMed: 12070305]
23. Tsuchiya Y, Nakabayashi O, Nakano H. FLIP the Switch: Regulation of Apoptosis and Necroptosis by cFLIP. Int J Mol Sci. 2015; 16:30321–30341. [PubMed: 26694384]
24. Daley JM, Thomay AA, Connolly MD, Reichner JS, Albina JE. Use of Ly6G-specific monoclonal antibody to deplete neutrophils in mice. J Leukoc Biol. 2008; 83:64–70. [PubMed: 17884993]
25. Brenner D, Blaser H, Mak TW. Regulation of tumour necrosis factor signalling: live or let die. Nat Rev Immunol. 2015; 15:362–374. [PubMed: 26008591]
26. Leibovich SJ, et al. Macrophage-induced angiogenesis is mediated by tumour necrosis factor-alpha. Nature. 1987; 329:630–632. [PubMed: 2443857]
27. Baluk P, et al. TNF-alpha drives remodeling of blood vessels and lymphatics in sustained airway inflammation in mice. J Clin Invest. 2009; 119:2954–2964. [PubMed: 19759514]
28. Espin R, et al. TNF receptors regulate vascular homeostasis in zebrafish through a caspase-8, caspase-2 and P53 apoptotic program that bypasses caspase-3. Dis Model Mech. 2013; 6:383–396. [PubMed: 22956347]
29. Asada N, et al. Differential cytokine contributions of perivascular haematopoietic stem cell niches. Nat Cell Biol. 2017
30. Eash KJ, Greenbaum AM, Gopalan PK, Link DC. CXCR2 and CXCR4 antagonistically regulate neutrophil trafficking from murine bone marrow. J Clin Invest. 2010; 120:2423–2431. [PubMed: 20516641]
31. Rezzoug F, et al. TNF-alpha is critical to facilitate hemopoietic stem cell engraftment and function. Journal of immunology. 2008; 180:49–57.
32. Grunewald M, et al. VEGF-induced adult neovascularization: recruitment, retention, and role of accessory cells. Cell. 2006; 124:175–189. [PubMed: 16413490]

33. Doan PL, et al. Epidermal growth factor regulates hematopoietic regeneration after radiation injury. Nature medicine. 2013; 19:295–304.
34. Pietras EM, et al. Functionally Distinct Subsets of Lineage-Biased Multipotent Progenitors Control Blood Production in Normal and Regenerative Conditions. Cell stem cell. 2015; 17:35–46. [PubMed: 26095048]
35. Pearl-Yafe M, et al. Tumor necrosis factor receptors support murine hematopoietic progenitor function in the early stages of engraftment. Stem cells. 2010; 28:1270–1280. [PubMed: 20506490]
36. Rebel VI, et al. Essential role for the p55 tumor necrosis factor receptor in regulating hematopoiesis at a stem cell level. The Journal of experimental medicine. 1999; 190:1493–1504. [PubMed: 10562323]
37. Pronk CJ, Veiby OP, Bryder D, Jacobsen SE. Tumor necrosis factor restricts hematopoietic stem cell activity in mice: involvement of two distinct receptors. The Journal of experimental medicine. 2011; 208:1563–1570. [PubMed: 21768269]
38. Ishida T, et al. Pre-Transplantation Blockade of TNF-alpha-Mediated Oxygen Species Accumulation Protects Hematopoietic Stem Cells. Stem cells. 2017; 35:989–1002. [PubMed: 27753160]
39. Lucas D, et al. Chemotherapy-induced bone marrow nerve injury impairs hematopoietic regeneration. Nature medicine. 2013; 19:695–703.
40. Galotto M, et al. Stromal damage as consequence of high-dose chemo/radiotherapy in bone marrow transplant recipients. Exp Hematol. 1999; 27:1460–1466. [PubMed: 10480437]
41. Schaefer BC, Schaefer ML, Kappler JW, Marrack P, Kedl RM. Observation of antigen-dependent CD8+ T-cell/ dendritic cell interactions in vivo. Cell Immunol. 2001; 214:110–122. [PubMed: 12088410]
42. Passegue E, Wagner EF, Weissman IL. JunB deficiency leads to a myeloproliferative disorder arising from hematopoietic stem cells. Cell. 2004; 119:431–443. [PubMed: 15507213]
43. Buch T, et al. A Cre-inducible diphtheria toxin receptor mediates cell lineage ablation after toxin administration. Nat Methods. 2005; 2:419–426. [PubMed: 15908920]
44. Pasparakis M, Alexopoulou L, Episkopou V, Kollias G. Immune and inflammatory responses in TNF alpha-deficient mice: a critical requirement for TNF alpha in the formation of primary B cell follicles, follicular dendritic cell networks and germinal centers, and in the maturation of the humoral immune response. The Journal of experimental medicine. 1996; 184:1397–1411. [PubMed: 8879212]
45. Peschon JJ, et al. TNF receptor-deficient mice reveal divergent roles for p55 and p75 in several models of inflammation. Journal of immunology. 1998; 160:943–952.
46. Lucas D, Battista M, Shi PA, Isola L, Frenette PS. Mobilized hematopoietic stem cell yield depends on species-specific circadian timing. Cell stem cell. 2008; 3:364–366. [PubMed: 18940728]
47. Mendez-Ferrer S, Lucas D, Battista M, Frenette PS. Haematopoietic stem cell release is regulated by circadian oscillations. Nature. 2008; 452:442–447. [PubMed: 18256599]
48. Puram RV, et al. Core Circadian Clock Genes Regulate Leukemia Stem Cells in AML. Cell. 2016; 165:303–316. [PubMed: 27058663]
49. Suire C, Brouard N, Hirschi K, Simmons PJ. Isolation of the stromal-vascular fraction of mouse bone marrow markedly enhances the yield of clonogenic stromal progenitors. Blood. 2012; 119:e86–95. [PubMed: 22262767]
50. Schindelin J, et al. Fiji: an open-source platform for biological-image analysis. Nat Methods. 2012; 9:676–682. [PubMed: 22743772]

In the bone marrow, granulocyte-derived TNFα acts on endothelial cells to maintain the vasculature under steady-state conditions and to promote its regeneration after injury or transplantation.

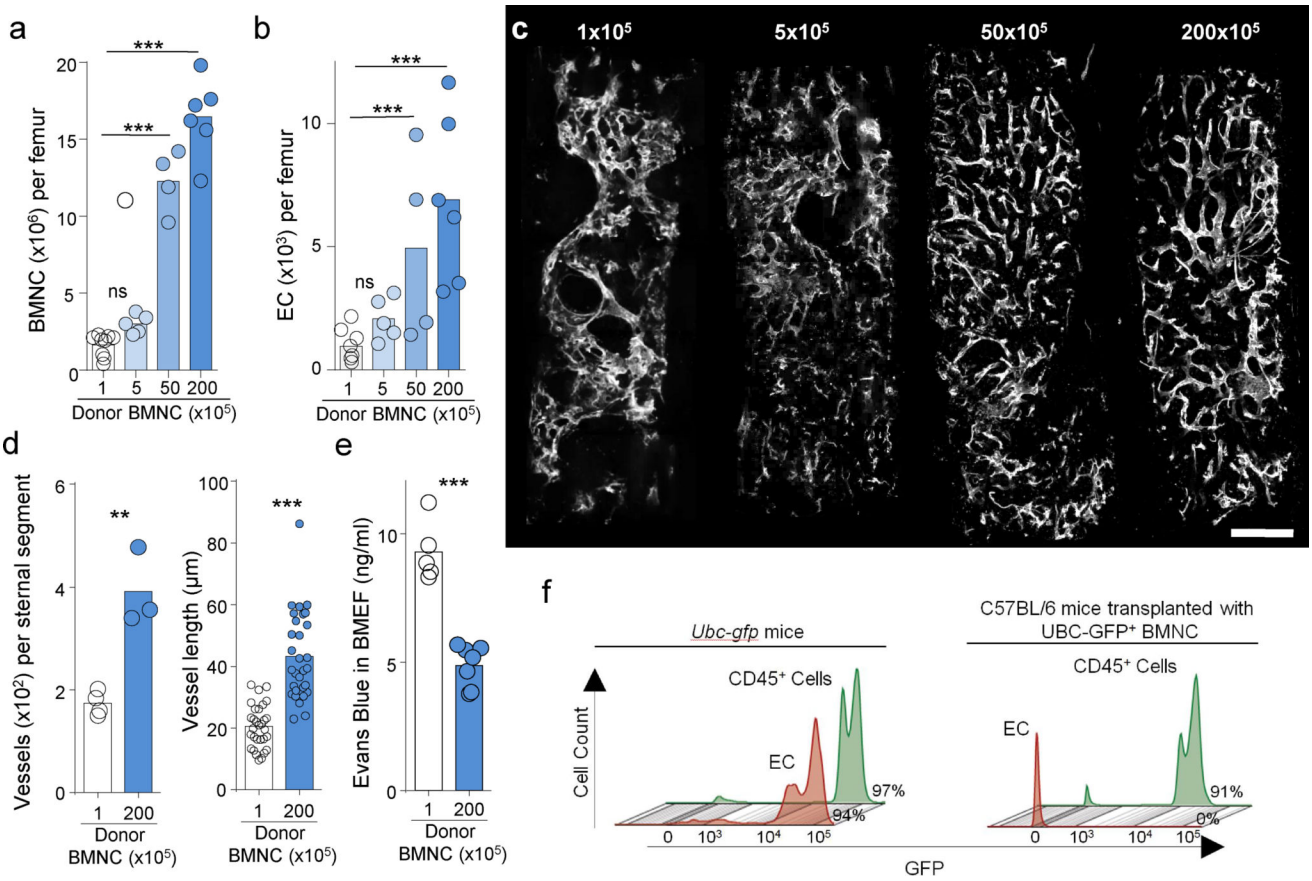

Figure 1. Donor hematopoietic cells drive endogenous vascular regeneration after transplantation

(**a,b**) The number of bone marrow nucleated cells (BMNC, **a**) and endothelial cells (EC, $CD45^{-}Ter119^{-}CD31^{+}CD105^{+}$, **b**) in the femur of B6-SJL mice 14 days after lethal irradiation and transplantion with the indicated numbers of $CD45.2^{+}$ BMNCs (1×10^{5}:n=8, 5×10^{5}: n=5, 50×10^{5}: n=4, 200×10^{5}: n=6). p-values were calculated using 1-way ANOVA model comparing the 3 higher doses to the lowest dose. Each circle represents one mouse. (**c**) A representative composite image showing blood vessels (white, CD31 and CD144) in the sternum of mice treated as in **a**. Scale bar 200μm. Images are representative of three mice for each group in two different experiments. (**d**) Quantification of intact blood vessel segments (left, each circle represents one mouse, 1×10^{5}: n=4 and 20×10^{5}: n=3) or average vessel length (right, each circle represents one vessel, 1×10^{5}: n=19 and 20×10^{5}: n=19) in the sternum of mice treated as in **a**. p-values were calculated using two tailed,Two-sample T-test. (**e**) Quantification of extravasation of Evans Blue dye in the BM extracellular fluid of mice treated as in **a**. (1×10^{5}: n=5 and 20×10^{5}: n=7). p-values were calculated using two tailed, Two-sample, T-test. (**f**) Percentage of GFP^{+} cells in FACS analyses of hematopoietic ($CD45^{+}$; gated as live,singlets, CD45+ cells) or endothelial cells (EC, gated as live, singlets, $CD45^{-}Ter119^{-}CD31^{+}CD105^{+}$ cells) in the BM of *Ubc-gfp* mice (left panel) or B6-SJL $CD45.1^{+}$ recipients transplanted with 20×10^{6} BMNCs purified from *Ubc-gfp* mice (right panel). The data shows representative FACS plots out of 3 mice per group in two

independent experiments. For all panels, bar graphs represent the mean and show the data of at least two independent experiments. *P<0.05, **P<0.01, ***P<0.001, n.s., not significant.

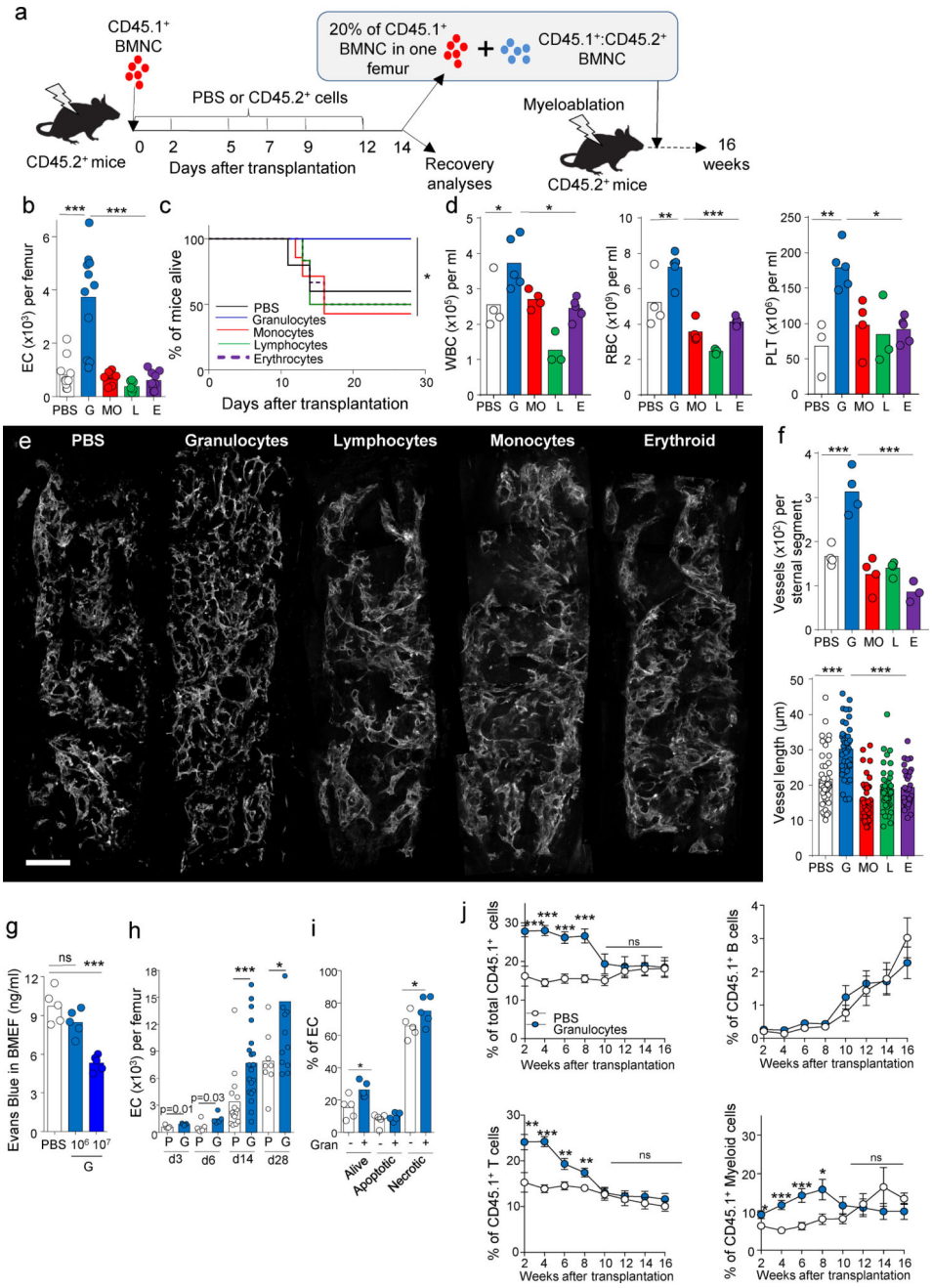

Figure 2. Granulocytes promote vascular regeneration

(**a**) Experimental design, CD45.2$^+$ recipients were lethally irradiated, followed by transplant of CD45.1$^+$ bone marrow nucleated cells (BMNC), and treatment with PBS or FACS-purified BM mature cells at the indicated time points. Mice were euthanized two weeks after the initial transplant and the BM and peripheral blood analyzed for regeneration. In some cases the CD45.1$^+$ cells were FASC purified, mixed with BMNC from CD45.1$^+$:CD45.2$^+$ mice and transplanted into lethally irradiated CD45.2$^+$ secondary recipients. (**b**) The number of endothelial cells (EC, CD45$^-$Ter119$^-$CD31$^+$CD105$^+$) in the femur of C57BL/6 mice 14 days after lethal irradiation and transplantation of 10^5 CD45.1$^+$ BMNCs, followed by

adoptive transfer of all of the granulocytes (G: $Gr1^+CD115^-$, 1×10^6), monocytes and macrophages (MO: $CD115^+$ or $F4/80^+$ cells pooled together cells within the $Gr1^-CD4^-CD8^-B220^-$ gate, 1×10^5), lymphocytes (L: $CD4^+$, $CD8^+$ and $B220^+$ cells pooled together , 7.5×10^5) and erythroid (E: $Ter119^+$, 1×10^5) cells found in 2×10^6 $CD45.2^+$ BMNCs (PBS n=11, G n=11, MO n=9, L n=8, E n=9). p-values were calculated using 1-way ANOVA model. (**c,d**) Survival curves (**c**, PBS n=5, G n=6, MO n=7, L n=6, E n=6) and peripheral blood recovery (**d**, PBS n=4, G n=5, MO n=4, L n=3, E n=5) for mice treated as in **b**; each circle represents one mouse. p-values were calculated using Log Rank analyses or one-way ANOVA. (**e**) A representative composite image showing blood vessels (white, CD31/CD144) in sternal segments purified from PBS-, G-, L-, MO- or E-treated mice 14 days after lethal irradiation and transplantation. Images are representative of four mice for each group in two different experiments. Scale bar 200μm. (**f**) Quantification of intact blood vessel segments (top, each circle represents one mouse; PBS: n=4, G: n=4, MO: n=4, L: n=4, E: n=3,) or average vessel length (bottom, each circle represents one vessel, PBS n=41, G n=40, MO n=40, L n=40, E n=30) in the sternum of the mice shown in **e**. p-values were calculated using one-way ANOVA. (**g**) Quantification of extravasation of Evans Blue dye in the BM extracellular fluid of transplanted mice treated with PBS (n=5) or serial adoptive transfer of 10^6 (n=5) or 10^7 granulocytes (n=5) 14 days after the initial transplant. p-values were calculated using one-way ANOVA. (**h**) Kinetics of endothelial cell recovery in PBS (P: D3 n=5, D6 n=5, D14 n=15, D28 n=8) or granulocyte (G: D3 n=5, D6 n=5, D14 n=20, D28 n=13) treated mice at the indicated time points. Each circle represents one mouse. p-values were calculated using two tailed, Two-sample, T-test. (**i**) Frequency of live, apoptotic and necrotic endothelial cells, determined using DAPI stain for live/death discrimination and caspase 3 staining to detect apoptotic and necrotic cells , in the BM of mice treated with PBS (n=5) or granulocytes (n=5) 6 days after transplantation. Each circle represents one mouse. p-values were calculated using two tailed, Two-sample, T-test. (**j**) $CD45.1^+$ cell engraftment in total, B, T or myeloid cells in secondary recipients at the indicated time points after transplantation of 2.5×10^5 $CD45.1^+$:$CD45.2^+$ competitor BMNCs and 20% $CD45.1^+$ cells obtained from one femur of granulocyte- or PBS-treated primary recipient mice 14 days after the primary transplant. PBS, n=18 for weeks 2–8, n=13 for weeks 10–16; Granulocytes n=17 for weeks 2–8, n=12 for weeks 10–16. p-values were calculated using two tailed, Two-sample, T-test. Dots indicate the mean and error bars the SEM. In all other panels the bar graphs represent the mean and show the pooled data of at least two independent experiments. *P<0.05, **P<0.01, ***P<0.001, n.s., not significant.

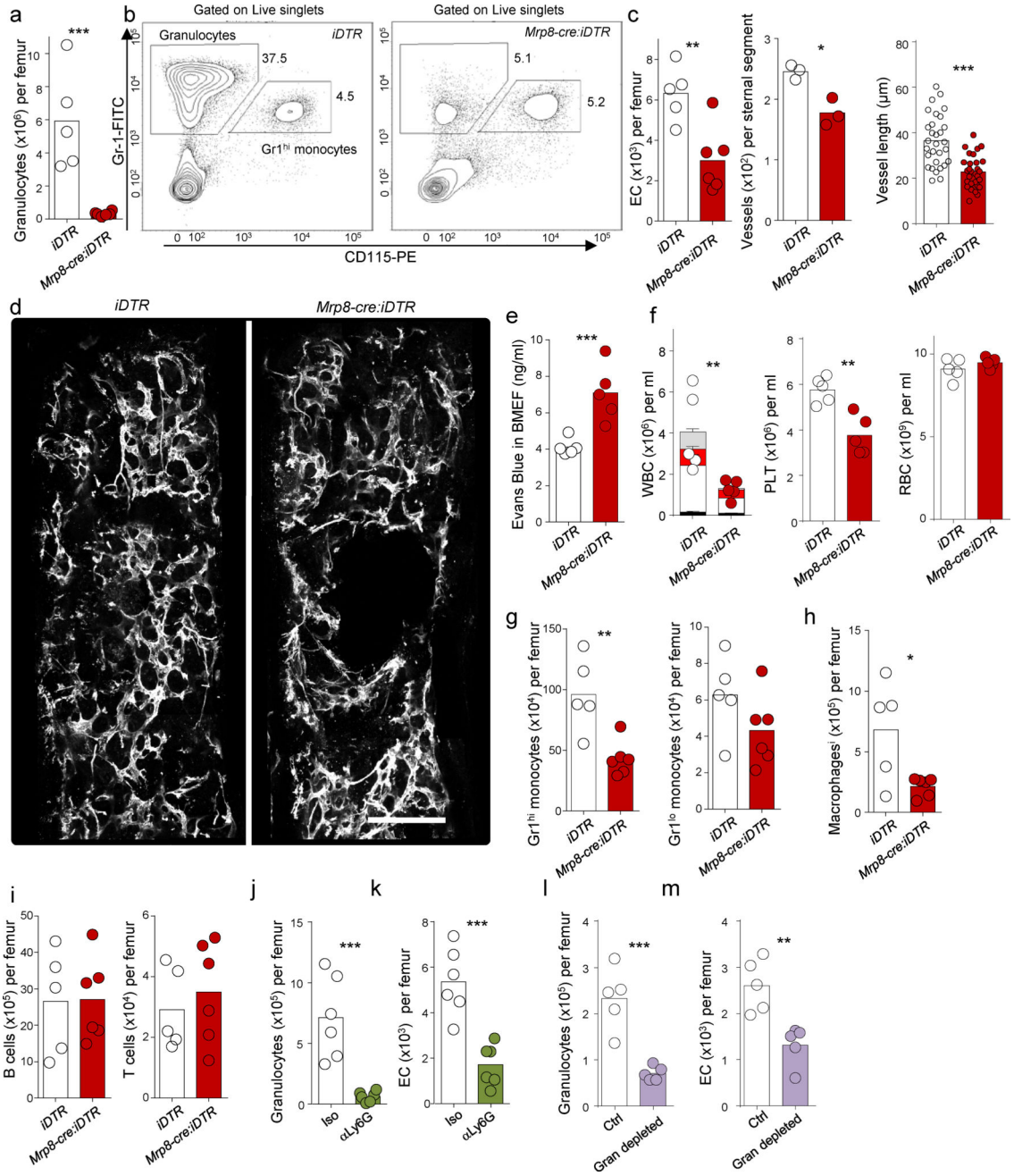

Figure 3. Granulocytes are necessary for vascular regeneration

(**a, b**) Quantification of the number of $Gr1^{+}CD115^{-}$ granulocytes (**a**) and representative FACS plots (**b**) in lethally irradiated C57BL6/J mice 14 days after transplantation of 5×10^{6} *iDTR* (n=5 mice) or *Mrp8-cre:iDTR* (n=6 mice) BMNCs, followed by diphtheria toxin treatment. FACS plots are representative of two experiments. (**c**) The number of endothelial cells (EC, $CD45^{-}Ter119^{-}CD31^{+}CD105^{+}$) in the femur (*iDTR*: n=5 mice, *Mrp8-Cre:iDTR*: n=6 mice) and the number (*iDTR*: n=3 mice, *Mrp8-Cre:iDTR*: n=3 mice) and length (*iDTR*: n=30 vessels from 3 mice, *Mrp8-Cre:iDTR*: n=30 vessels from 3 mice) of vessels in the sternum of the mice analyzed in **a**. (**d**) A representative composite image showing blood

vessels (white, CD31/CD144) in sternal segments of C57BL/6J mice treated as in **a**. Images are representative of 3 mice per group in two different experiments. Scale bar 200μm. (**e**) Quantification of extravasation of Evans Blue dye in the BM extracellular fluid of mice treated as in **a** (*iDTR*: n=5, *Mrp8-Cre:iDTR*: n=5). (**f**) Number of white blood cells (each circle represents one mouse) and frequency of T cells (black bar), B cells (white bar), monocytes (red bar) and neutrophils (grey bar) (left); platelets (middle) and red blood cells (right) in the peripheral blood of mice treated as in **a**. (*iDTR*: n=5, *Mrp8-Cre:iDTR*: n=5). (**g-i**) Numbers of monocytes (**g**), macrophages (**h**), and lymphocytes (**i**) in the BM of the mice treated as in **a**. (*iDTR*: n=5, *Mrp8-Cre:iDTR*: n=6) (**j,k**) Numbers of $Ly6G^+$ granulocytes (j) and endothelial cells (k) in the BM of lethally irradiated C57BL6/J mice 6 days after transplantation of 10^6 BMNC and treatment with isotype control (Iso; n=6) or αLy6G antibodies (n=6). (**l,m**) Numbers of granulocytes (**l**) and endothelial cells (**m**) in the BM of lethally irradiated C57BL6/J mice 6 days after transplantation of 10^6 BMNC (Ctrl: n=5) or a graft of 0.5×10^6 BMNCs containing all other hematopoietic cells found in 10^6 BMNC but in which granulocytes had been removed via FACS (Gran depleted: n=5). For all panels p-values were calculated using two tailed, Two-sample, T-test and the graphs show the pooled data of at least two independent experiments. Bar graphs represent the mean and error bars represent standard error. *P<0.05, **P<0.01, ***P<0.001, n.s., not significant.

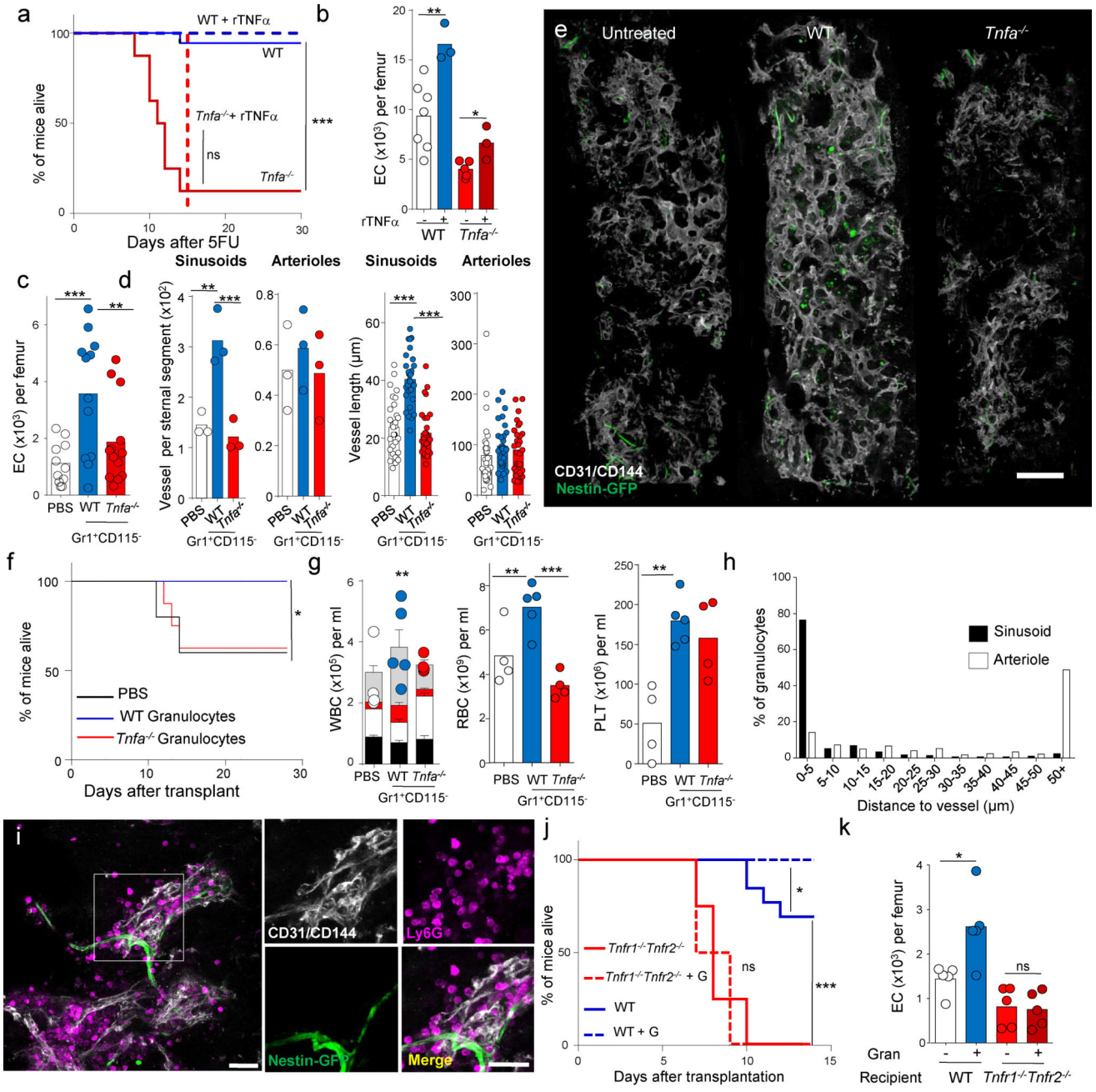

Figure 4. Granulocytes promote vascular regeneration via TNFα

(**a**) Survival curves for WT and *Tnfa*$^{-/-}$ mice after injection of 250mg/kg body weight of 5-fluorouracil (5FU) and treatment with either PBS (WT n=18, *Tnfa*$^{-/-}$ n=16) or recombinant TNFα (WT n=7, *Tnfa*$^{-/-}$ n=4). p-values were calculated using Log Rank analyses. (**b**) Number of endothelial cells in the femur of C57BL/6 mice treated as in **a**, 8 days after 5FU injection. (WT-r TNFα: n=7, WT+rTNFα: n=3, *Tnfa*$^{-/-}$-rTNFα: n=5, *Tnfa*$^{-/-}$+rTNFα: n=3). p-values were calculated using two tailed, Two-sample T-test. (**c**) Number of endothelial cells in the femurs of *Nestin-gfp* mice 14 days after lethal irradiation and transplantation of 10^5 CD45.1$^+$ BMNCs, followed by treatment with PBS (n=11) or adoptive

transfer of $Gr1^+CD115^+$ granulocytes from WT (n=12) or *Tnfa*$^{-/-}$ (n=13) mice. p-values were calculated using 1-way ANOVA model. (**d**) Quantification of the number (each circle represents one mouse. PBS: n=3, WT: n=3, *Tnfa*$^{-/-}$: n=3) and length (each circle represents one vessel, PBS: n=90, WT: n=90 and *Tnfa*$^{-/-}$: n=90 vessels from 3 mice) of intact sinusoidal and arterial segments in the sternum of the mice shown in **c**. p-values were calculated using 1-way ANOVA model. (**e**) A representative composite image showing blood vessels (white, CD31/CD144) in sternal segments of *Nestin-gfp* mice treated with PBS (untreated), WT or *Tnfa*$^{-/-}$ granulocytes. Images are representative of at least 5 mice per group in four different experiments Scale bar=200μm (**f**) Survival curves for the mice treated as in c (PBS n=5, WT n=6, *Tnfa*$^{-/-}$ n=8). (**g**) Number of white blood cells (each circle represents one mouse) and frequency of T cells (black bar), B cells (white bar), monocytes (red bar) and neutrophils (grey bar) (left); platelets (middle) and red blood cells (right) in the peripheral blood of mice treated as in **c**. (PBS: n=4, WT: n=5, *Tnfa*$^{-/-}$: n=4). p-values were calculated using 1-way ANOVA model. (**h**) Percentage of granulocytes (n=305 granulocytes in two mice) found at the indicated distances from sinusoids (black) or arterioles (white) in *Nestin-gfp* mice 6 days after lethal irradiation and transplantation of 10^6 BMNCs. Bar graphs represent the pooled data of two mice in two independent experiments. (**i**) Immunofluorescence analyses showing the association between transferred granulocytes (magenta, Ly6G) with regenerating sinusoids (white, CD31/CD144) and arterioles (white and green, CD31/CD144$^+$Nestin-GFP^{bright}) in the mice shown in **h**. Scale bar=25μm. Images are representative from 2 mice in two independent experiments. (**j**) Survival curves for WT and *Tnfr1*$^{-/-}$*:Tnfr2*$^{-/-}$ mice after lethal irradiation and transplantation of 10^5 $CD45.1^+$ BMNCs, followed by treatment with PBS (WT n=13, *Tnfr1*$^{-/-}$*:Tnfr2*$^{-/-}$ n=4) or adoptive transfer of WT granulocytes (WT n=12, *Tnfr1*$^{-/-}$*:Tnfr2*$^{-/-}$ n=6). p-values were calculated using Log Rank analyses. (**k**) Number of endothelial cells in mice treated as in j but 6 days after the initial transplant. (WT+PBS: n=5, WT+Gran: n=5, *Tnfr1*$^{-/-}$*:Tnfr2*$^{-/-}$+PBS: n=5, *Tnfr1*$^{-/-}$*:Tnfr2*$^{-/-}$+Gran: n=5). p-values were calculated using 1-way ANOVA model. In all panels (with the exception of h) the graphs show the pooled data of at least two independent experiments and bar graphs represent the mean. Error bars represent the standard error. *P<0.05, **P<0.01, ***P<0.001, n.s., not significant.